Quantum Electronics **49** (9) 887 – 893 (2019)

https://doi.org/10.1070/QEL17022

Recording of pulsed currents by a fibre-optic Faraday effect-based sensor with limited frequency band

V.P. Gubin, N.I. Starostin, Ya.V. Przhiyalkovsky, S.K. Morshnev, A.I. Sazonov

Abstract. **We have studied, experimentally and theoretically, the dependence of the amplitude and noise response parameters of a fibre-optic Faraday effect-based current sensor on the photodetector frequency band in recording rectangular current pulses, the duration of which does not exceed the time of light propagation through the sensing fibre. The presence of an optimal band at which the signal-to-noise ratio has a pronounced maximum is demonstrated. It is shown that the optimal bandwidth is close in magnitude to the inverse time of light passage through the fibre. The revealed feature is explained by the difference in dependences of the response amplitude and the white noise level of optical radiation on the frequency band of the photodetector. A technique for amplitude error correction at the optimal band is proposed.**

Keywords: *Faraday effect, fibre-optic current sensor, photorecording band, signal-to-noise ratio.*

1. Introduction

Interest in the use of interferometric fibre-optic electric current sensors (FOCS's) based on the Faraday effect [1 – 4] for measuring short-duration pulse currents [5 – 7] is due to the low inertia of the effect (~ 1 ns) and the practical advantages of these sensors. Particularly, FOCS's do not require break in the wireway of the current being measured, are convenient in installation and operation, and their sensing elements can be located at remote and hazardous facilities.

The principle of FOCS operation is based on the magnetic-field-induced Faraday phase shift current between orthogonal circularly polarised light waves in an optical sensing fibre wound around the current wire. The interference of these waves at the output of the FOCS optical circuit converts the phase shift into a change in the radiation intensity recorded by the photodetector. As a result, a response to the measured current is formed at the photodetector output.

The shape of the response of such fibre-optic sensors to a rectangular current pulse is an isosceles trapezium [7]. A similar shape occurs in the case of a sufficiently wide photorecording band, comparable to the spectral width of the measured pulse and at least significantly exceeding the inverse time of light propagation through the fibre loop (the time-of-flight effect). On the other hand, with a wide photorecording band required to record short current pulses, the light noise level inherent in optical sensors increases significantly, which limits the possibility for recording small-amplitude current pulses. Noise in sensors employing low-coherent optical radiation from super-luminescent light sources is represented by two components [8]: photonic (shot) noise caused by the discrete nature of light, and excess noise arising from the beatings of broadband light components. Both components result in light intensity noise having a uniform spectral density (white noise). With increasing radiation power on the photodetector (from several μW), the main contribution to this noise is made by the excess noise of low coherent radiation, the value of which increases in proportion to the radiation power at the photodetector. Therefore, when recording current pulses under these conditions, the search for ways to increase the signal-to-noise ratio is relevant. One of possible solutions is to narrow the photorecording band (optimal band). Given that the response shape is distorted by narrowing the frequency band, and its maximum value is reduced, the selection criteria may be the attainment of the maximum signal-to-noise ratio and allowable value of the amplitude measurement error.

In this work, we study the FOCS response to a rectangular current pulse in a large range of the photorecording band values (photodetector). The main attention is paid to the recording of pulses the duration of which does not exceed the time light passage through the sensing fibre. The justification for the selection criteria of the current sensor band in recording of such pulses is the aim of this work.

2. Calculations

The main element of the Faraday effect-based FOCS is a sensing fibre loop consisting of one or more turns of a magnetically sensing fibre and enveloping a conductor with a measured current [1 – 4]. The optical scheme of the sensor may be transmissive or reflective. In the first case, a polariser and an analyser are installed at the input and output of the sensing loop, respectively. In the second case, a single polariser is employed at the loop input, and a reflector is installed at the loop output. Both optical schemes can be used in high-speed current sensors. One of the main factors that impose a restriction on the sensor speed, which leads to a distortion in the response shape, is the transit time of radiation along the loop (time-of-flight effect) [5 – 7]. Another factor may be the band of the electronic signal processing system, particularly the photodetector band.

Next, we consider the recording of rectangular current pulses [7]. The radiation intensity at the output of the optical sensor scheme (sensor response) repeats the Faraday phase

V.P. Gubin, N.I. Starostin, Ya.V. Przhiyalkovsky, S.K. Morshnev, A.I. Sazonov Kotelnikov Institute of Radio Engineering and Electronics (Fryazino Branch), Russian Academy of Sciences, prosp. Vvedenskogo 1, 141190 Fryazino, Moscow region, Russia; e-mail: nistar53@mail.ru

Received 22 March 2019; revision received 22 May 2019
Kvantovaya Elektronika **49** (9) 887 – 893 (2019)
Translated by M.A. Monastyrskiy

shift between the orthogonally polarised light waves, which is induced by the current being measured.

Let a rectangular current pulse with the amplitude I_0 have the duration T_c, and the light propagation time along the sensing fibre loop be equal to T_t. For the case when the photorecording band significantly exceeds $1/T_t$, the response shapes $H(t), h(t)$ to a rectangular current pulse with the amplitude I_0 are shown in Fig. 1 [7]. We emphasise that in this case the response shape is only determined by the time-of-flight effect. The following parameters were taken as an example: T_t = 1 μs, T_c = 1.5, 1.0, and 0.5 μs. The response has the shape of an isosceles trapezoid, the parameters of which depend on the ratio between T_c and T_t (the isosceles triangle is a special case of a trapezoid). The trapezoid height H_0 (response amplitude) at $T_c \geqslant T_t$ corresponds to the Faraday phase shift $\Delta\varphi_F$ at a constant current equal to I_0:

$$\Delta\varphi_F = H_0 = aVSN_1N_2I_0, \tag{1}$$

where $a = 2(4)$ for the transmissive (reflective) optical scheme; $V = 7 \times 10^{-7}$ A W^{-1} is the Verdet constant for fused silica; $S \approx 1$ is the relative magneto-optical sensitivity of the fibre in the loop; N_1 is the number of turns of fibre in the loop; and N_2 is the number of turns of the wire with the measured current passing through the loop's plane.

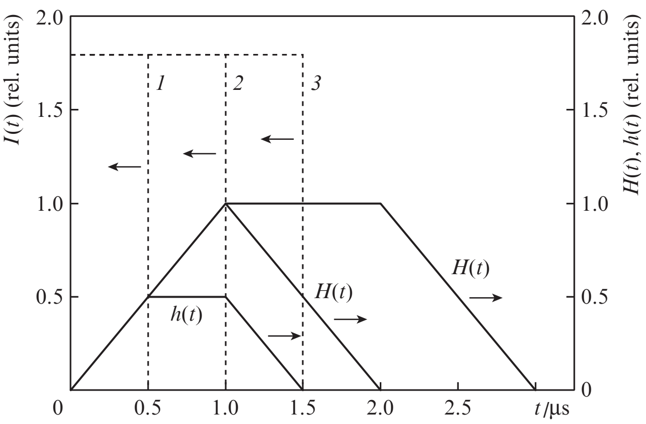

Figure 1. Theoretical response shapes $H(t)$ and $h(t)$ for various current pulse durations $I(t)$ at an infinitely wide photodetector band ($T_{ph} = 0$): T_c = (*1*) 0.5, (*2*) 1, and (*3*) 1.5 μs. The response $h(t)$ corresponds to T_c = 0.5 μs, and the responses $H(t)$ – to 1 and 1.5 μs. Time-of-flight is T_t = 1 μs.

At the inverse ratio ($T_c < T_t$), the response amplitude $h(t)$, while maintaining the trapezoidal shape, decreases to h_0 (see Fig. 1) [7]:

$$h_0 = H_0T_c/T_t. \tag{2}$$

The leading and trailing edges of the trapezoid are linear functions, with a slope proportional to the current amplitude. Their duration does not exceed the time-of-flight. The transition to a flat top is abrupt, with no smooth establishing process.

It follows from formula (2) that, in the case $T_c < T_t$, it is possible to determine the true maximum value of the current pulse proportional to H_0, if the current pulse duration T_c is known:

$$H_0 = h_0T_t/T_c. \tag{3}$$

It should be noted that expression (3) is valid for a rectangular current pulse; however, as shown in [6], in the case of a pulse of arbitrary shape, it is also possible to obtain a calculated relation for H_0 if the amplitude h_0 and the pulse duration are known.

2.1. Method for calculating the shape of the response to a rectangular pulse with account for the photorecording band

As follows from the above, the signal $U_s(t)$ at the photodetector output (pulse response voltage) for a sufficiently wide (theoretically infinite) photodetector band has a shape similar to that shown in Fig. 1. It is assumed that the light-detecting photodetector includes a low-inertia photodiode, a photocurrent–voltage conversion microcircuit, and a low-pass filter with a single pole (integrating RC circuit), which has a time constant $T_{ph} = R_{ph}C_{ph}$ (R_{ph} is a load resistor, and C_{ph} is a shunt capacitor). In this case, the photodetector frequency band is $\Delta F = 1/(2\pi R_{ph}C_{ph})$. The output signal $U_s(t)$ is generated at the low-pass filter output.

Consider the effect of the photodetector time constant T_{ph} on the output signal shape (sensor response) if the current pulse duration $T_c \leqslant T_t$. It is in the case of short pulses that it is important to increase the signal-to-noise ratio by narrowing the photodetector band.

Figure 2 shows the calculated response to a short current pulse with parameters T_c = 0.25 μs, T_{ph} = 0.6 μs, T_t = 1 μs. The method for calculating the response shape at $T_c \leqslant T_t$ is given below. The expression for the response shape is a solution to the first-order differential equation for the voltage $U_s(t)$ of the low-pass filter output at the input voltage $U_{in}(t)$:

$$T_{ph}\mathrm{d}U_s(t)/\mathrm{d}t + U_s(t) = U_{in}(t). \tag{4}$$

The solution for the input signal $U_{in}(t)$ in the trapezoid form is described by the relations

$$U_{in}(t) = kt, \quad U_s(t) = kt - kT_{ph}(1 - \exp(-t/T_{ph})),$$
$$0 < t < t_1, \tag{5}$$

$$U_{in}(t) = h_0, \quad U_s(t) = h_0(1 - \exp(-t/T_{ph})) - C_1\exp(-t/T_{ph}),$$
$$t_1 < t < t_2, \tag{6}$$

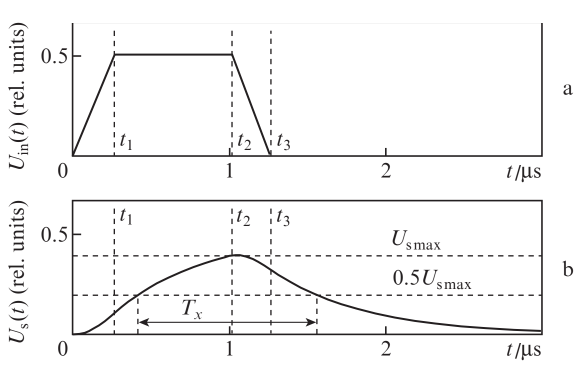

Figure 2. Current sensor response to a rectangular current pulse: (a) voltage at the RC-filter input; (b) voltage at the RC-filter output. T_c = 0.25 μs, T_t = 1 μs, T_{ph} = 0.6 μs.

$$U_{\rm in}(t) = A - kt, \quad U_{\rm s}(t) = A - kt + kT_{\rm ph}(1 - \exp(-t/T_{\rm ph}))$$

$$- C_2\exp(-t/T_{\rm ph}), \quad t_2 < t < t_3, \tag{7}$$

$$U_{\rm in}(t) = 0, \quad U_{\rm s}(t) = C_3\exp(-t/T_{\rm ph}), \quad t > t_3, \tag{8}$$

where C_i are the integration constants (selected to 'sew' the segments); h_0 is the trapezoid top (in this example, $h_0 = 0.5$); k is the rate of rise (decline) of the input signal (here $k = 2$ μs^{-1}); and A is a constant ($A = 2.5$). From (5)–(8), we determine the response amplitude $U_{\rm s\,max}$ and the FWHM duration T_x (see Fig. 2). In our case, the maximum output signal voltage is $U_{\rm s\,max} = 0.388$ at the input voltage $h_0 = 0.5$; the output signal FWHM duration is $T_x = 1.143$ μs.

As already mentioned, as $T_{\rm ph}$ increases, an amplitude error occurs when determining the maximum current pulse, equal to ~ 0.3 at $T_{\rm ph}/T_{\rm t} \approx 0.6$. The amplitude error is systematic and can be account for or excluded when processing the signal with the response area calculation.

Integrating (4) in time, we obtain

$$T_{\rm ph}U_{\rm s}(t)\Big|_{-\infty}^{+\infty} + \int U_{\rm s}(t)\,{\rm d}t = \int U_{\rm in}(t)\,{\rm d}t = Q. \tag{9}$$

The function $U_{\rm s}(t)$ in (9) is a bounded function, i.e., $U_{\rm s}(t \to +\infty) \to 0$. Therefore, in the case of a bounded response function, the first term in (9) vanishes, the area Q under the response curve $U_{\rm s}(t)$ (see Fig. 2) does not depend on the photodetector time constant and is equal to the trapezoid area (FOCS response at an infinite photodetector band, see Fig. 1):

$$Q = \int_0^\infty H(t)\,{\rm d}t = H_0T_{\rm c}, \quad T_{\rm c} \geqslant T_{\rm t}, \tag{10}$$

$$Q = \int_0^\infty h(t)\,{\rm d}t = h_0T_{\rm t} = H_0T_{\rm c}, \quad T_{\rm c} < T_{\rm t}. \tag{11}$$

Given that, according to (10) and (11), the trapezoid area (FOCS response at an infinite photodetector band) is expressed in terms of $T_{\rm c}$ and $T_{\rm t}$, one can claim that the independence on $T_{\rm ph}$ of the area under the response curve takes place for any possible ratios between $T_{\rm c}$ and $T_{\rm t}$.

Thus, by calculating Q according to (11), we can restore the true value of H_0. Note that for the case $T_{\rm c} > T_{\rm t}$, this procedure using (10) is also applicable.

2.2. Calculating the response shape and parameters

Using the technique described above, we calculate the response shape for the time constant range $T_{\rm ph} = 0.1$–1.5 μs of the photodetector. The current pulse duration $T_{\rm c}$ is selected within an arbitrary range of 0.25–1.0 μs, for which the condition $T_{\rm c} \leqslant T_{\rm t}$ is satisfied. Figure 3 shows the current shape $I(t)$ and the response $U_{\rm s}(t)$ for $T_{\rm c} = 1$ μs (Fig. 3a) and $T_{\rm c} = 0.25$ μs (Fig. 3b) for various values of the photodetector time constant $T_{\rm ph}$. The time-of-flight in these cases is $T_{\rm t} = 1$ μs. It is seen that, with increasing $T_{\rm ph}$, the maximum response value $U_{\rm s\,max}$ decreases, and its FWHM duration T_x increases.

Next, consider the dependence of the response parameters $U_{\rm s\,max}$ and T_x on the photodetector time constant $T_{\rm ph}$ referred to the time-of-flight ($T_{\rm ph}/T_{\rm t}$). We represent these parameters in a normalised form, taking as a unity the parameter value at

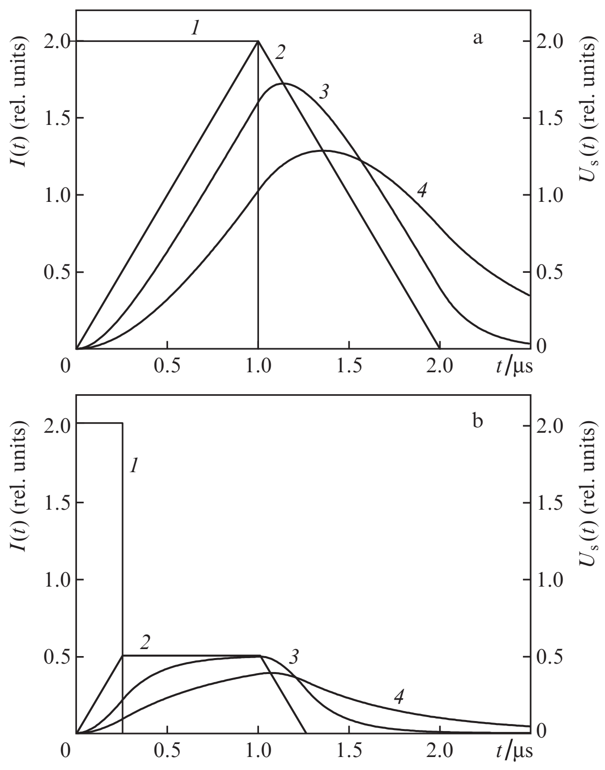

Figure 3. Calculated FOCS response $U_{\rm s}(t)$ to current pulses $I(t)$ (*1*) with duration $T_{\rm c} = 1$ (a) 1 μs and (b) 0.25 μs at $T_{\rm ph} = 0$ (*2*) 0, (*3*) 0.2, and (*4*) 0.6 μs.

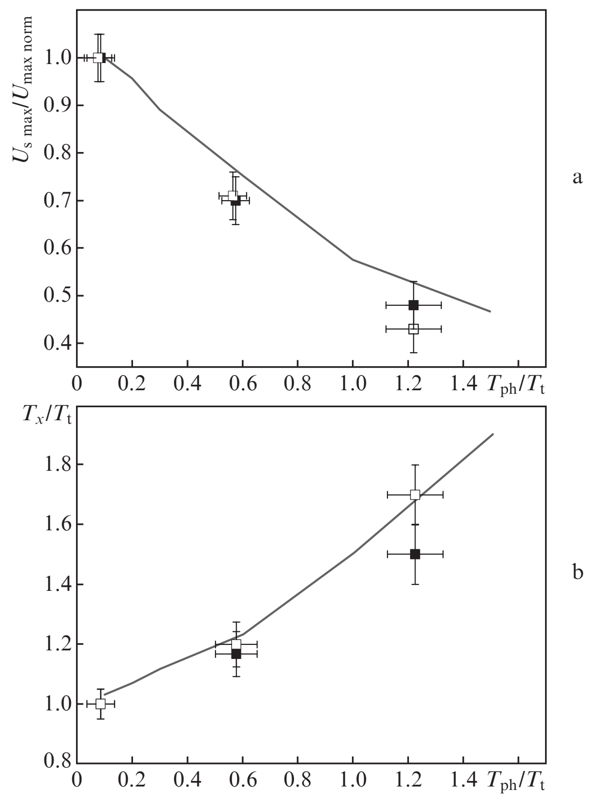

Figure 4. Calculated (solid curves) and experimental (dots) dependences of the normalised response parameters (a) $U_{\rm s\,max}$ and (b) T_x on the normalised photodetector time constant $T_{\rm ph}/T_{\rm t}$ at current pulse durations $T_{\rm c}/T_{\rm t}$ = (■) 1.0 and (□) 0.25. In the calculations, $T_{\rm c}/T_{\rm t} = 0.25$–$1.0$.

a small time constant $T_{ph} = 0.1$ μs. Figure 4 shows the dependence of the normalised response parameters $U_{s\,max}$ and T_x on the normalised time constant T_{ph}/T_t of the photodetector at various current pulse durations T_c/T_t.

2.3. Signal-to-noise ratio analysis

As was noted in the Introduction, noises in the optical current sensor are determined by photon (shot) noise and the noise of spectral beatings of a broadband light source (excess noise) [8]. These noises have a uniform spectral density (white noise) within the operating frequency band of the sensor and are additive, summing up with the operating signal. They reduce the accuracy of measuring the low-amplitude current pulses and limit the sensor detectivity (threshold sensitivity).

The estimated root mean-square value of the noise voltage at the photodetector output is determined by the relation

$$U_n = \{B[2ePqR_{ph}^2 + (PqR_{ph}\lambda)^2(1/(c\Delta\lambda)) + 4kTR_{ph}]\}^{1/2}. \quad (12)$$

Here, the first term describes the photonic noise $U_{n\,sh}$, the second term is the excess noise of light $U_{n\,ex}$, and the third term is the thermal noise $U_{n\,th}$ of the resistor, which exceeds the noise of the photodetector microcircuit. The filter noise band B for the RC circuit is defined as $B = (\pi/2)\Delta F$. The following parameters were taken for calculations: $R_{ph} = 12.5$ kΩ, $\Delta F = 1.8$ MHz, e is the electron charge, $P = 30$ μW is the light power on the photodiode, $q = 1$ A W^{-1} is the photodiode quantum efficiency, $\lambda = 1550$ nm is the average wavelength of the light source, $\Delta\lambda = 20$ nm is the spectrum width of the light source, c is the speed of light in vacuum, k is the Boltzmann constant, and $T = 290$ K is the temperature. Calculation by formula (12) gives $U_n = 0.32$ mV, $U_{n\,ex} = 0.32$ mV, $U_{n\,sh} = 0.05$ mV, and $U_{n\,th} = 0.02$ mV. Therefore, due its key contribution, we only consider excess noise in (12).

Let us calculate the signal-to-noise ratio as a function of the photodetector time constant T_{ph}. As the signal U_s of the pulse current sensor, it is advisable to choose the maximum value $U_{s\max}$ of the photodetector output signal (see Fig. 2), which, as noted above, is proportional to H_0 or h_0 (response amplitude at $T_{ph} = 0$).To represent $U_{s\max}$ as a function of the sensor parameters, we use the output characteristic of the interferometer in the form given in [9]:

$$U_s = U_0[1 + K\cos(\Delta\varphi_F + \pi/2 + G)], \quad (13)$$

where $U_0 = PqR_{ph}$ is the average voltage at the photodetector output; K is the contrast (visibility) of the interferometer; and G is the operating point shift relative to $\pi/2$.

In the case of small shifts ($\Delta\varphi_F \ll 1$), under the condition $G \ll 1$ and with allowance for the decrease in response due to the impact of the low-pass filter, with the use of (13) we obtain the expression for the signal:

$$U_{s\max} = k_{ph}PqR_{ph}K\Delta\varphi_F, \quad (14)$$

where $k_{ph} = U_{s\max}/U_{\max\,norm} \leqslant 1$ is the coefficient accounting for a reduction in the response amplitude at the low-pass filter output with an increase in the time constant T_{ph}, determined by the dependence shown in Fig. 4a. Then, with allowance for (14), (12), and (1), the signal-to-noise ratio $r = U_{s\max}/U_n$ as a function of the photodetector time constant has the form

$$r = \alpha k_{ph}[(\pi/2)\Delta F]^{-1/2}, \quad (15)$$

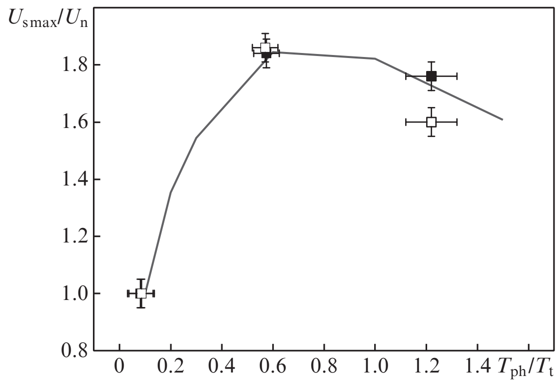

Figure 5. Calculated (solid curve) and experimental (dots) dependences of the normalised signal-to-noise ratio on the normalised photodetector time constant T_{ph}/T_t at current pulse durations T_c/T_t = (■) 1.0 and (□) 0.25. In the calculations, $T_c/T_t = 0.25-1.0$.

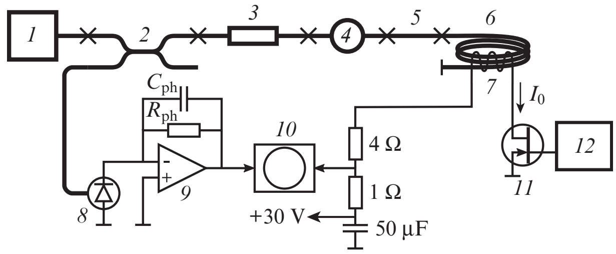

Figure 6. Experimental setup:
(*1*) radiation source; (*2*) directional coupler; (*3*) polariser; (*4*) Faraday discrete rotator; (*5*) connecting line; (*6*) sensing loop; (*7*) solenoid; (*8*) photodiode; (*9*) photodetector with variable bandwidth; (R_{ph}) resistor; (C_{ph}) capacitor for bandwidth selection; (*10*) double-beam oscilloscope; (*11*) pulse current amplifier; (*12*) master oscillator.

where $\alpha = K\Delta\varphi_F(c\Delta\lambda)^{1/2}/\lambda$. In the framework of our problem, α is a constant.

It is advisable to represent the signal-to-noise ratio in relative units and in a normalised form, since we are interested in the form of the function $r(T_{ph}/T_t)$ (Fig. 5). For normalisation, the value of r at $T_{ph}/T_t = 0.1$ is taken as a unity. It is seen that the signal-to-noise ratio has a maximum at $T_{ph}/T_t \approx 0.6$. The existence of a maximum in the dependence $r(T_{ph}/T_t)$ in the region of short pulses $T_c/T_t \leqslant 1$ is stipulated by the fact that the functions of the signal $U_{s\max}(T_{ph}/T_t)$ and noise $U_n(T_{ph}/T_t)$ decrease monotonically with increasing T_{ph}; however, the rate of their change depends on T_{ph} in different ways. Thus, the signal at first changes slowly, and then begins to drop almost linearly, whereas the noise in the entire specified region decreases inversely with respect to $\sqrt{T_{ph}}$. This behaviour of the functions leads to the appearance of a maximum in their ratio at $T_{ph\,opt} \approx 0.6T_t$. The value of $T_{ph\,opt}$ is not accidentally close to the sensor's time-of-flight T_t determined by the fibre length of the sensing loop, since, in this range of T_{ph}/T_t values, a linear decrease in the signal with increasing T_{ph}/T_t has already been established (see Fig. 4a).

3. Experiment

The functional diagram of the experimental setup is shown in Fig. 6. The setup is a reflective low-coherence fibre interferometer with the recording of the Faraday phase shift induced by the current being measured, without the use of auxiliary

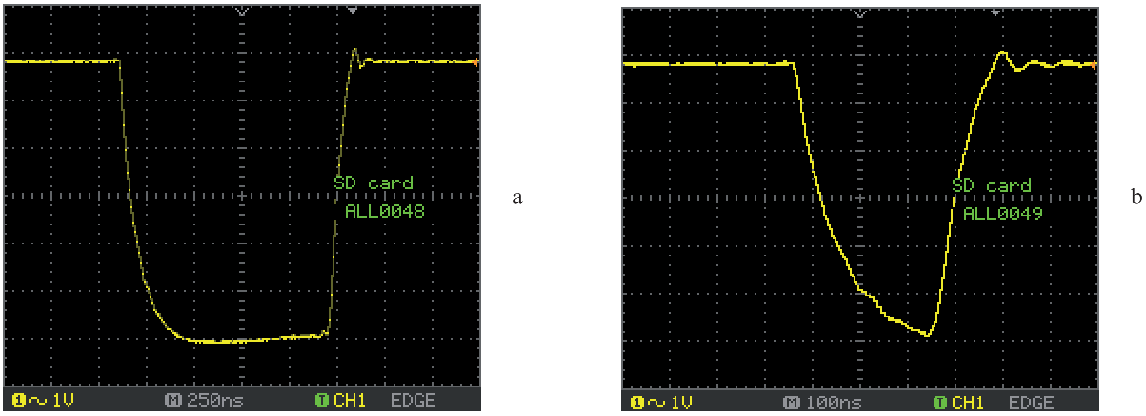

Figure 7. Oscillograms of current pulses used in the experiment: (a) $I_0 = 6$ A, $T_c = 1.1$ µs; (b) $I_0 = 6$ A, $T_c = 0.275$ µs.

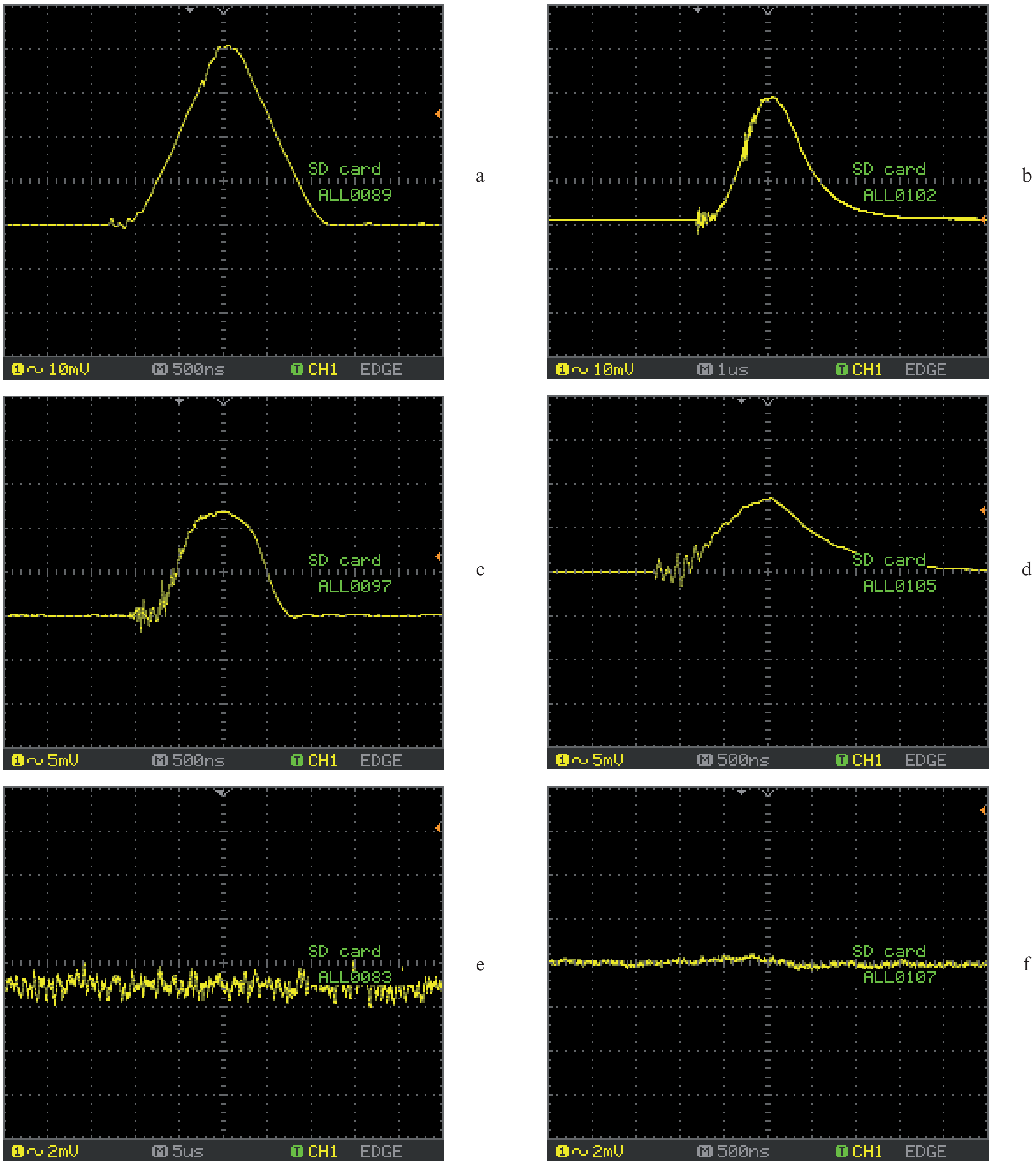

Figure 8. FOCS response $U_s(t)$ (a–d) and noise $U_n(t)$ (e–f) oscillograms at (a) $T_c = 1100$ ns, $T_{ph} = 88$ ns; (b) $T_c = 1100$ ns, $T_{ph} = 625$ ns; (c) $T_c = 275$ ns, $T_{ph} = 88$ ns; (d) $T_c = 275$ ns, $T_{ph} = 625$ ns; (e) $T_{ph} = 88$ ns and (f) $T_{ph} = 625$ ns.

phase modulation of light. The interferometer includes a superluminescent fibre radiation source (*1*) with a centre wavelength of 1550 nm and a spectrum width of 20 nm, a directional coupler (*2*), a fibre polariser (*3*), a discrete Faraday rotator (*4*), a connecting line (*5*), and a sensing fibre loop (*6*) with a Fresnel mirror at the end. Elements (*5*) and (*6*) are made of spun fibre with a beat length of the built-in linear birefringence $L_b = 10$ mm and a spiral pitch $L_{sp} = 3$ mm. The interferometer operating point was determined by a constant phase shift of 90°, formed by the rotator (*4*). The output signal of the interferometer was detected by a photodiode (*8*) connected to the input of the transimpedance cascade (*9*). The sensing loop (*6*) was a multi-turn spun fibre loop (number of turns $N_1 = 2000$) wound on the mandrel with an initial winding diameter of 14 mm. The estimated time of double passage of light for this loop was $T_t = 1100$ ns.

The sensor output signal proportional to the Faraday shift $\Delta\varphi_F$ was taken from the output of the transimpedance cascade (*9*) (photodetector) with a passband determined by the load elements R_{ph} and C_{ph}, and recorded on the oscilloscope screen (*10*). The linearisation of the interferometer characteristic was not performed because the signals corresponded to small values of $\Delta\varphi_F$ (about 0.2 rad). To control the amplitude distortion of the response, the amplitude of the pulse signals was compared with a dc signal. The measured maximum bandwidth of the photodetector was $\Delta F = 1.8$ MHz at a resistor resistance $R_{ph} = 12.5$ kΩ (minimum time constant $T_{ph} = 1/(2\pi\Delta F) = 88$ ns).

To increase the response, the current pulse being measured was passed through a solenoid 7 made of a copper wire with the number of turns $N_2 = 5$ wound around a sensing fibre loop. The current pulses T_c were formed using the FDD6635 field-effect transistor with an amplitude of 6 A at durations of 1.1 and 0.275 μs (Fig. 7).

Figure 8 shows the FOCS response to the above current pulses for two values of the photodetector time constant. The results of measurements of the response parameters for the time constant $T_t = 1.1$ μs are given in Table 1.

Table 1.

Pulse duration/μs	Response parameters				
	T_{ph}/μs	$U_{s\,max}$/mV	T_x/μs	U_n (RMS)/mV	r
$T_c = 1.1$	0.089	40	1.13	0.33	121
	0.625	28	1.36	0.13	215
	1.34	19	1.80	0.09	211
$T_c = 0.275$	0.089	12	1.10	0.33	36
	0.625	8.5	1.2	0.13	65
	1.34	5.2	1.7	0.09	58

We should note that the root mean-square (RMS) of the noise here was estimated by the oscillogram under the assumption that the total noise amplitude corresponded to the sum of six RMS's. The optimal photorecording bandwidth ΔF_{opt} constituted 255 kHz.

4. Discussion of the results

Analysis of the calculated and experimental results presented in Figs 4, 5, 8 and Table 1 allows us to conclude that they are in good qualitative and satisfactory quantitative agreement. From these results it follows that the relative values of the response parameters $U_{s\,max}$ and T_x for different photodetector time constants T_{ph} are determined by the value of T_{ph} and do not virtually depend on the current pulse duration T_c. It should be emphasised that this property is peculiar to the studied range of current duration T_c, which are equal to or less than the time-of-flight of light along the loop: $T_c = (0.25-1.0)T_t$.

Another important conclusion is the presence of a maximum in the signal-to-noise ratio at a certain time constant T_{ph}/T_t, which in the specified T_c range is approximately equal to 0.6. The signal-to-noise ratio can be increased up to two times. It should be noted that this conclusion was obtained under the condition that the change in capacitance C_{ph} to narrow the passband (to increase T_{ph}) was performed with the fixed resistance R_{ph} of the photodiode load resistor. Meanwhile, the signal-to-noise ratio in the photodetector scheme under consideration can be additionally enhanced by increasing R_{ph} at the lowest possible value of C_{ph} determined by the assembly capacitance. This follows from relation (15): $r \sim 1/\sqrt{\Delta F} \sim \sqrt{R_{ph}}$. In the scheme under consideration, an additional 2.5-fold increase in r is possible, i.e., the total increase in the signal-to-noise ratio will be about five times.

We should also note that the indicated values of r were obtained by arbitrarily setting the initial wide band (minimum time constant $T_{ph}/T_t = 0.1$), at which the distortions were considered acceptable.

Evaluation of r in absolute units using formula (15) for the parameters of this work and $T_{ph} = 0.625$ μs yielded the following results: $r = 207$ at $T_c = 1.1$ μs, $k_{ph} = 0.75$, $a = 4$, $V = 7 \times 10^{-7}$ rad A^{-1}, $S = 1.23$, $K = 0.6$, $\Delta\lambda = 20$ nm, $\lambda = 1.55$ μm, $I_0 = 6$ A, and $T_t = 1.1$ μs. This estimate is consistent with the experimental data: $r = 215$ (see Table 1). With a four-fold decrease in the pulse duration ($T_c = 0.275$ μs), the experimentally measured response amplitude and the value of r turned out to be 3.3 times smaller than those at $T_c = 1.1$ μs. It should be noted that for an inertia-free photorecording system ($T_{ph} = 0$) [7] at a given ratio of pulse durations, the results should differ four times (this is true for a current pulse of rectangular shape).

In the conditions of this experiment, for $T_c = 1.1$ μs, the minimum detectable current (FOCS detectability) is $I_{0\,min} = I_0/r = 30$ mA. In accordance with the foregoing, as the pulse duration decreases, the threshold value of $I_{0\,min}$ increases by a close-to-linear law.

To improve the detectability of broadband FOCS's, a further search is needed for ways to increase the signal-to-noise ratio when recording low-amplitude current pulses in the nanosecond range. One of the ways to solve this problem may be the use of new optical FOCS schemes with suppression of excess noise and sensing fibres with an increased Verdet constant.

5. Conclusions

We have experimentally and theoretically studied the dependence of the amplitude and noise parameters of the response of a Faraday effect-based fibre-optic current sensor on the frequency band of a photodetector when recording rectangular current pulses. The case of short current pulses whose duration does not exceed the propagation time of radiation along the sensing loop is considered. It is in this case that it is important to increase the signal-to-noise ratio, in particular, by reducing the photodetector frequency band. The presence of an optimal photorecording band at which the signal-to-noise ratio has a pronounced maximum is demonstrated. In this case, the optimal band width is close in magnitude to the inverse time of the passage of light through the fibre. The revealed feature is explained by the difference in the dependence of the response amplitude and the amount of white noise of optical radiation on the photodetector frequency band. The maximum increase in the signal-to-noise ratio when selecting the optimal band can reach two or more times in comparison with the photorecording regime, in which the response shape distortions associated with the photodetector band are small. A technique for correcting the amplitude error at the optimal band is proposed. Another advantage of the proposed approach is a significant reduction in the requirements for operating speed of a photoelectron recording unit. The results of this work can be used in the development of the broadband FOCS's designated for recording pulse currents.

References

1. Laming R.I., Payne D.N. *J. Lightwave Technol.*, **7** (12), 2084 (1989).
2. Blake J., Tantaswadi P., De Carvalho R.T. *IEEE Transactions on Power Delivery*, **11** (1), 116 (1996).
3. Bohnert K., Gabus P., Kostovic J., Brandle H. *Opt. Lasers Eng.*, **43** (3), 511 (2005).
4. Gubin V.P., Isaev V.A., Morshnev S.K., Sazonov A.I., Starostin N.I., Chamorovsky Yu.K., Oussov A.I. *Quantum Electron.*, **36** (3), 287 (2006) [*Kvantovaya Elektron.*, **36** (3), 287 (2006)].
5. Kersey A.D., Bucholtz F., Dandridge A. *Int. J. Optoelectron.*, **3** (4), 323 (1988).
6. Chen G.Y., Newson N.P. *Electron. Lett.*, **50** (8), 626 (2014).
7. Przhiyalkovsky Yu.V., Gubin V.P., Starostin N.I., Morshnev S.K., Sazonov A.I. *Quantum Electron.*, **48** (1), 62 (2018) [*Kvantovaya Elektron.*, **48** (1), 62 (2018)].
8. Burns W.K., Moeller R.P., Dandridge A. *IEEE Photon. Technol. Lett.*, **2** (8), 606 (1990).
9. Gubin V.P., Morshnev S.K., Starostin N.I., Chamorovsky Y.K., Sazonov A.I., Przhiyalkovsky Yu.V., Boev A.I. *Quantum Electron.*, 41 (9), 815 (2011) [*Kvantovaya Elektron.*, **41** (9), 815 (2011)].